

Study of Two-Proton States of the ^{20}Ne Nucleus by $(^3\text{He}, n)$ Reaction

著者	Fujii Y., Tohei T., Nakagawa T., Narita A., Hino T., Orihara H., Ishii K., Terakawa A., Hosaka M., Guan Z., Ito K., Teramoto Y., Yamamoto A., Abe K., Suehiro T., Ohnuma H.
journal or publication title	CYRIC annual report
volume	1994
page range	1-5
year	1994
URL	http://hdl.handle.net/10097/49809

I. 1. Study of Two-Proton States of the ^{20}Ne Nucleus by (^3He , n) Reaction

*Fujii Y., Tohei T., Nakagawa T., Narita A.****, Hino T.,
Orihara H.*, Ishii K.*, Terakawa A.*, Hosaka M.*****, Guan Z.*,
Ito K., Teramoto Y., Yamamoto A.*, Abe K.**, Suehiro T.***,
and Ohnuma H.*****

*Department of Physics, Tohoku University
Cyclotron and Radioisotope Center, Tohoku University *
Department of Nuclear Engineering, Tohoku University **
Tohoku Institute of Technology ***
Department of Physics, Tokyo Institute of Technology ****
Faculty of Science, Hirosaki University *****
Institute for Nuclear Study, University of Tokyo ******

Two-nucleon transfer reactions by light ions are expected to excite states of two particle configuration selectively, if they proceed with a direct reaction process. There are many measurements for two-neutron or proton-neutron transfer reactions at present, but relatively little information is available for a two-proton transfer reaction like (^3He ,n), which has been mainly accomplished at low incident energies.

Two-proton states of the ^{20}Ne nucleus have been studied through the $^{18}\text{O}(^3\text{He},\text{n})$ reaction at 18MeV¹⁾. However, this energy is not enough high to proceed mainly through a direct reaction and observed angular distributions of the cross section have not been distinguished clearly for transitions with large transfer momenta. Therefore, the incident energy of 30MeV was selected to make the direct reaction more dominant.

The experiment was carried out using a 30MeV ^3He beam from the AVF cyclotron at the Cyclotron and Radioisotope Center, Tohoku University. Neutron energies were measured by a time-of-flight (TOF) technique²⁾. Twelve neutron detectors of 5cm thickness filled with liquid scintillator NE213 were located at 35m from the target, where the effective detection solid angle was 0.37msr. Angular distributions of emitted neutrons were measured at laboratory angles between 0° to 45° using a beam-swinger system. ^{18}O gas isotopically enriched to 98.0% was used as a target. The gas was contained in two types of gas cells, disk typed and cylindrical ones. Target thickness was ranged from 1.9 to 3.2mg/cm².

The excitation energy range up to 23MeV were covered in the present measurements and angular distributions of the differential cross sections were obtained for 27 peaks. Typical overall time resolution was 2.0ns, which corresponded to the energy resolution of 600keV for the ground state transition. In Table 1, excitation energies and spin-parities for

observed peaks are shown together with the results of Evers et al.¹⁾ and the compilation by Ajzenberg-Selove³⁾ for states which the correspondence is well established (except for the state at 18.37MeV).

Finite-range distorted-wave Born-approximation (DWBA) calculations for the differential cross section have been accomplished with the code DWUCK5⁴⁾. The potential parameters for the entrance and exit channels were taken from systematic ones of Becchetti & Greenlees⁵⁾ and Watson et al.⁶⁾, respectively. Spectroscopic amplitudes employed in the DWBA calculations were obtained from a shell-model calculation with the code OXBASH⁷⁾, using full sd-shell effective interactions of Wildenthal⁸⁾. Negative parity states have been calculated with a pure ($1f_{7/2}, 1d_{5/2}$) configuration.

In Figure 1, typical experimental angular distributions are shown together with DWBA predictions. The theoretical curves have been normalized to the data. The DWBA calculations well reproduce the experimental angular distributions for the seven states with well-known spin-parities, but one for 5.68MeV 1^- state fails to reproduce the data. From the comparison of the DWBA predictions with the data, new spin-parities are tentatively proposed for four peaks at 8.52, 9.08, 10.67 and 18.37MeV, and two spin-parity candidates for other seven peaks as shown in Table 1. For the peaks at 8.52 and 9.08MeV, corresponding states have not been reported yet. Though the DWBA calculation for the peak at 18.37MeV cannot exclude 3^- , we would be able tentatively to identify the peak as the 18.43MeV first $T=2$, 2^+ state, because this peak is strongly excited and only the angular distribution shape of this peak shows one for low spin state around this excitation energy in the present measurement.

In Table 2, obtained enhancement factors are listed with these for ^{16}O , $^{40,42,44}\text{Ca}(^3\text{He},n)$ reactions obtained by our group^{9,10)}. In the table a tendency is seen that enhancement factors for the 0^+ states are greater than these for the 2^+ and 4^+ states. From our results, one can guess that typical enhancement factors for the DWBA analysis using DWUCK5 are about 8 for the 0^+ states and 3 for the 2^+ , 4^+ states.

Analyses taking account a sequential transfer $^3\text{He}-d-n$ process have been also carried out within the framework of the second order DWBA calculation with the code TWOFNR¹¹⁾. The potential parameters for intermediate channels were taken from systematic ones of Daehnick et al.¹²⁾ Spectroscopic amplitudes for the ($^3\text{He},d$) and (d,n) steps were also obtained from the above described shell model calculation, and 11 states of ^{19}F were employed as the intermediate channels. In Figure 2, the direct ($^3\text{He},n$) term (dotted), sequential $^3\text{He}-d-n$ term (broken) and coherent sum of them (solid) are displayed without any normalization to the data. The present results of the calculations indicate that contributions from sequential transfer process are important for the two nucleon transfer reaction cross section and the fits of the angular shape to the data become rather worse by the inclusion of the present sequential transfer process. However, there are some remaining problems in the present work. Especially the used optical potential parameters were selected to reproduce

experimental angular distributions by one step term only. So the parameters may include the effect of the sequential transfer term, already. Other problems may be on the three body wave function used in the present analyses and on the neglected non-orthogonal term of the sequential transfer process. Further discussions for these problems are in progress.

References

- 1) Evers D. et al., Nucl. Phys. **A275** (1977) 363.
- 2) Orihara H. et al., Nucl. Instr. and Meth. **A257** (1987) 189.
- 3) Ajzenberg-selove F., Nucl. Phys. **A475** (1984) 1.
- 4) Kunz P. D., DWBA code DWUCK5, unpublished.
- 5) Becchetti F. D., Jr. and Greenlees W., Polarization Phenomena in Nuclear Reactions. The University of Wisconsin Press, Madison, Wis (1971).
- 6) Watson B. A., Singh P. P. and Segel R. E. Phys. Rev. **182** (1969) 977.
- 7) Etchegoyen A., Rae W. D. M. and Godwin N. S., Shell Model Code OXBASH, unpublished.
- 8) Wildenthal B. H., Prog. Part. Nucl. Phys. **11** (1984) 5.
- 9) Hosomi K. et al., CYRIC Annual Report (1991) 5.
- 10) Narita A. et al., CYRIC Annual Report (1993) 16.
- 11) Igarashi M., DWBA code TWOFNR, unpublished.
- 12) Daehnick W. W., Childs J. D. and Vrcelj Z., Phys. Rev. **C21** (1980) 2253.

Table 1. Excitation energies and spin-parities for the present observed peaks.

Present		Ajzenberg-selove ³⁾		Evers et.al. ¹⁾	
$E_x(\text{MeV})$	J^π	$E_x(\text{MeV})$	J^π	$E_x(\text{MeV})$	J^π
0.00	0^+	0.0	0^+	0.0	0^+
1.61	2^+	1.6337	2^+	1.65	2^+
4.24	4^+	4.2477	4^+	4.21	4^+
5.68	1^-	5.6214	1^-	5.71	1^-
		6.725	0^+	6.72	0^+
7.17	3^-	7.1563	3^-	7.15	3^-
8.52	4^+				
				(8.74)	
9.08	1^-				
10.14	$2^+; 1$	10.274	$2^+; 1$	10.24	$2^+; 1$
10.67	4^+			10.83	
11.17					
				11.48	(0^+)
12.23	$2^+; 1$	12.221	$2^+; 1$	12.21	$2^+; 1$
12.86	$(2^+, 4^+)$				
13.59	$(2^+, 4^+)$			13.57	(2^+)
14.01	$(3^-, 4^+)$			13.93	(2^+)
14.57					
15.00				(15.1)	
15.58	$(3^-, 4^+)$			15.52	$(2^+; 1)$
16.09	$(2^+, 3^-)$			16.01	$(2^+; 1)$
16.76	$0^+; 2$	16.732	$0^+; 2$	16.73	$0^+; 2$
17.69				17.55	$(2^+; 1)$
				17.91	(0^+)
18.37	$2^+; 2$	18.430	$2^+; 2$		
19.33				19.33	
19.88	$(2^+, 3^-)$				
20.75					
21.60					
22.36	$(2^+, 3^-)$				
22.95					

Table 2. Enhancement factors for well known states near the ground states obtained with DWBA analyses using DWUCK5 together with the results of the other works.

	^{20}Ne 30MeV*	$^{18}\text{Ne } (9)$ 30MeV*	$^{18}\text{Ne } (9)$ 45MeV*	$^{42}\text{Ti } (10)$ 50MeV*	$^{44}\text{Ti } (10)$ 50MeV*	$^{46}\text{Ti } (10)$ 50MeV*
0_1^+	8.6	3.3	2.8	6.0	11	14
2_1^+	3.1	1.9	1.9	2.9	2.6	3.6
4_1^+	4.0	2.1	1.8	2.8	2.6	3.1
6_1^+	-	-	-	3.5	5.9	7.4
$2_1^+; 1$	6.6					
$2_2^+; 1$	4.1					
$0_1^+; 2$	15.5					
$2_1^+; 2$	6.3					

* Incident energy

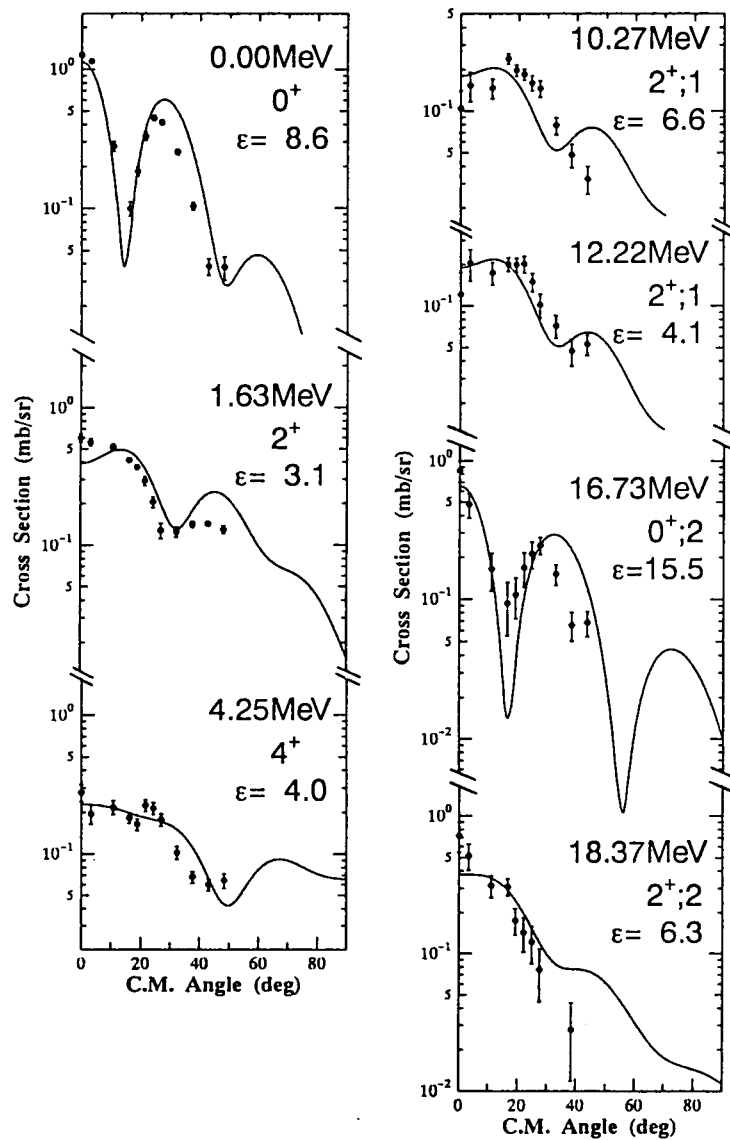


Fig. 1. Typical angular distributions obtained in the $^{18}\text{O}(\text{He},n)^{20}\text{Ne}$ reaction at 30MeV. Curves represent the DWBA predictions by DWUCK5. The theoretical curves have been normalized to the data.

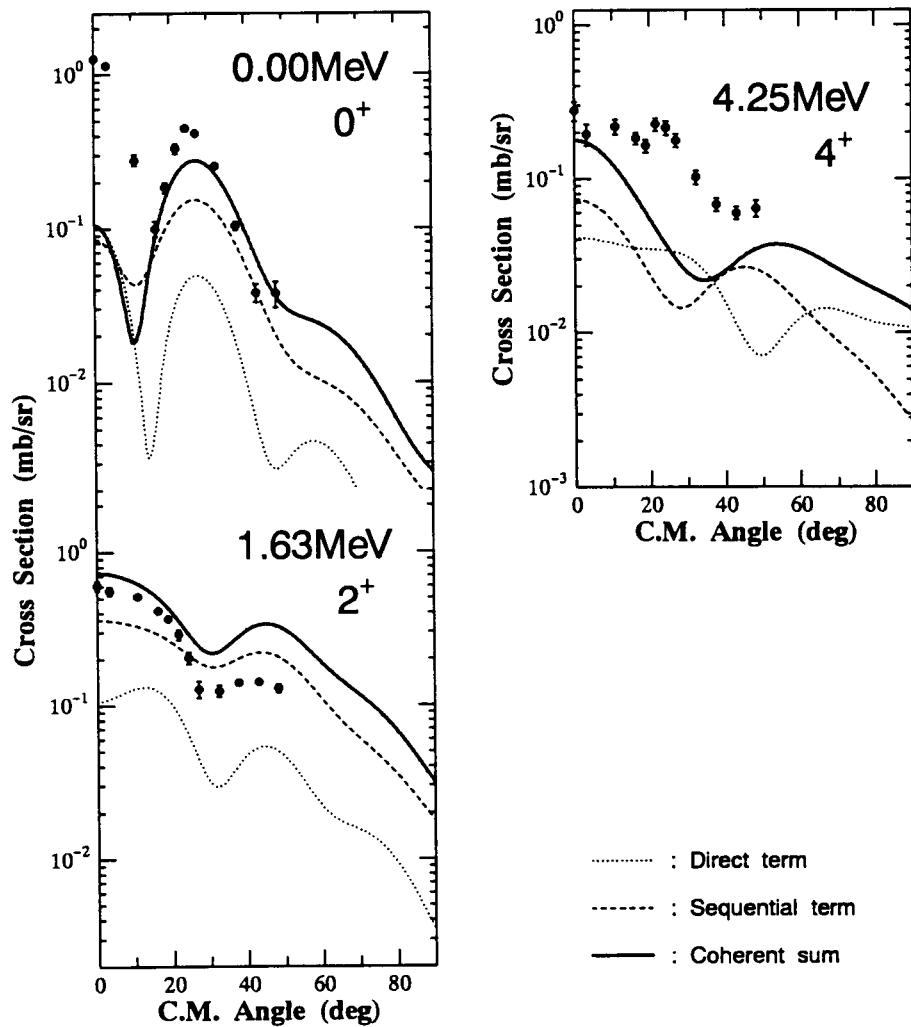


Fig. 2. Angular distributions and DWBA predictions by TWOFNDR for the 0^+_{1} , 2^+_{1} and 4^+_{1} states. Dotted and broken curves represent the direct term and sequential term, respectively, and solid curves represent the coherent sum of them. The curves are displayed without any normalization.